



Cite this: *New J. Chem.*, 2015, **39**, 7656

One ligand fits all: lanthanide and actinide sandwich complexes comprising the 1,4-bis(trimethylsilyl)cyclooctatetraenyl (=COT^{''}) ligand†‡

Janek Rausch,^a Christos Apostolidis,^{*b} Olaf Walter,^b Volker Lorenz,^a Cristian G. Hrib,^a Liane Hilfert,^a Marcel Kühling,^a Sabine Busse^a and Frank T. Edelmann^{*a}

The series of anionic lanthanide(III) sandwich complexes of the type [Ln(COT^{''})₂]⁻ (COT^{''} = 1,4-bis(trimethylsilyl)cyclooctatetraenyl dianion) has been largely extended by the synthesis of eight new derivatives ranging from lanthanum to lutetium. The new compounds [Li(DME)₃][Ln(COT^{''})₂] (Ln = Y (**1**), La (**2**), Pr (**3**), Gd (**4**), Tm (**6**), Lu (**8**)) and [Li(THF)₄][Ln(COT^{''})₂] (Ln = Ho (**5**), Tm (**7**)) were prepared in good yields following a straightforward synthetic protocol which involves the treatment of LnCl₃ with 2 equiv. of *in situ*-prepared Li₂COT^{''} in either DME (=1,2-dimethoxyethane) or THF. The neutral actinide sandwich complexes An(COT^{''})₂ (An = Th (**9**), U (**10**)) and An(COT^{'''})₂ (COT^{'''} = 1,3,6-tris(trimethylsilyl)cyclooctatetraenyl dianion; An = Th (**11**), U (**12**)) were synthesized in a similar manner, starting from ThCl₄ or UCl₄, respectively. The COT^{''} ligand imparts excellent solubility even in low-polar solvents as well as excellent crystallinity to all new compounds studied. All twelve new f-element sandwich complexes have been structurally authenticated by single-crystal X-ray diffraction. All are nearly perfect sandwich complexes with little deviation from the coplanar arrangement of the substituted COT^{''} rings. Surprisingly, all six [Li(DME)₃][Ln(COT^{''})₂] complexes covering the entire range of Ln³⁺ ionic radii from La³⁺ to Lu³⁺ are isostructural (space group *P*1̄). Compound **10** is the first uranocene derivative for which ¹³C NMR data are reported.

Received (in Montpellier, France)
21st April 2015,
Accepted 3rd June 2015

DOI: 10.1039/c5nj00991j

www.rsc.org/njc

1. Introduction

Second only to the omnipresent cyclopentadienyl complexes, the dianionic 10π-cyclooctatetraenyl ligand C₈H₈²⁻, commonly abbreviated as COT, plays an important role in the organometallic chemistry of lanthanides and actinides for almost 50 years. There is a general understanding that the large, flat C₈H₈²⁻ ring is ideally suited for overlapping with the f-orbitals of the large lanthanide and actinide ions.¹ Early work in this area was mainly focused on complexes bearing unsubstituted COT ligands.² Scheme 1 shows some prototypical lanthanide COT complexes which are considered milestones in the development of organolanthanide chemistry using COT ligands.

Notable are the anionic sandwich complexes K[Ln(COT)₂] (**A**),³ the dimeric half-sandwich mono(cyclooctatetraenyl)-lanthanide chlorides [(COT)Ln(μ-Cl)(THF)₂]₂ (**B**),⁴ the mixed-sandwich complexes (COT)LnCp (**C**),⁵ and the so-called cerocene, Ce(COT)₂ (**D**).⁶ The chemistry of such lanthanide COT complexes has already been summarized in several comprehensive review articles.^{2,7}

In the case of actinides, the discovery of uranocene, U(COT)₂ (Scheme 2, An = U), by Streitwieser and Müller-Westerhoff in 1968 had a considerable impact on the development of organoactinide chemistry.^{11,12} Following the preparation of uranocene, other tetravalent actinidocenes An(C₈H₈)₂ (Scheme 2; An = Th, Pa, Np, Pu) have also been reported.¹² The bonding in uranocene is considered to be less ionic than in the lanthanide sandwich complexes K[Ln(COT)₂] (**A**) and Ce(COT)₂ (**D**). Uranocene is also significantly more stable than cerocene and the thorium analogue Th(COT)₂, which can be explained by a higher degree of covalency due to a stronger participation of the 5f and 6d orbitals in the uranium-cyclooctatetraenyl bonding. Recent work by Ephritikhine and co-workers has demonstrated that the chemistry of actinidocenes continues to produce very interesting results.¹³

In general, the use of the unsubstituted COT ligand in organo-lanthanide and -actinide chemistry has several disadvantages

^a *Chemisches Institut der Otto-von-Guericke-Universität Magdeburg, Universitätsplatz 2, 39106 Magdeburg, Germany.*

E-mail: frank.edelmann@ovgu.de; Fax: +49 391 6712933; Tel: +49 391 6758327

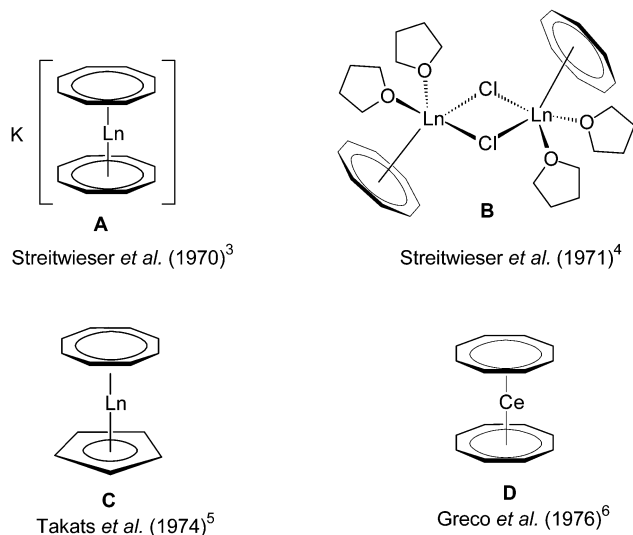
^b *European Commission, Joint Research Centre, Institute for Transuranium Elements, P.O. Box 2340, 76125 Karlsruhe, Germany.*

E-mail: christos.apostolidis@ec.europa.eu

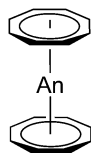
† Dedicated to Professor Basil Kanellakopulos on the occasion of his 80th birthday.

‡ CCDC 1052366–1052372 (**1–8**) and 1049924–1049927 (**9–12**). For crystallographic data in CIF or other electronic format see DOI: 10.1039/c5nj00991j





Scheme 1 Prototypical lanthanide COT sandwich and half-sandwich complexes.



An = Th, Pa, U, Np, Pu

Scheme 2 Schematic representation of the neutral actinidocenes An(C₈H₈)₂ (An = Th, Pa, U, Np, Pu).

in terms of low solubility and/or poor crystallinity. For example, the most important series of precursors in lanthanide COT chemistry, the chloro-bridged mono(COT) dimers [(COT)Ln(μ-Cl)(THF)₂]₂ (Scheme 1, **B**),⁴ lack good solubility even in THF. Moreover, commercially available cyclooctatetraene is very expensive. As a consequence, more soluble alternative starting materials such as (COT)LnI(THF)_n (Ln = Tm, n = 2; Ln = La, Ce, Pr, Nd, Sm, n = 3)^{2,8} and [(COT)Ln(μ-O₃SCF₃)(THF)]₂ (Ln = Ce, Pr, Nd, Sm)⁹ have been reported in the literature, but their use as precursors in organolanthanide chemistry still remains limited.² More recently, lanthanide COT chemistry received fundamental new impulses through the use of bulky silyl-substituted cyclooctatetraenyl ligands. The initial idea originated from the pioneering work of Cloke *et al.*, who first employed the 1,4-bis(trimethylsilyl)cyclooctatetraenyl dianion (=COT^{''}) in organo-f-element chemistry.¹⁰ In many cases, using the bulky COT^{''} ligand did in fact improve the solubility of the products, but occasionally also led to novel molecular structures and coordination geometries.^{7g,10,14} Typical examples include the unprecedented cluster-centered Pr/Li multidecker sandwich complex of the composition [Pr(COT^{''})]₂[Pr₂(COT^{''})₂]₂Li₂(THF)₂Cl₈¹⁵ as well as the first linear rare-earth metal triple-decker complexes Ln₂(COT^{''})₃ (Ln = Nd, Gd, Dy, Ho, Er).^{14,16–18} Previously reported anionic lanthanide sandwich complexes comprising [Ln(COT^{''})₂][−] anions include the THF solvates [Li(THF)₄][Ln(COT^{''})₂] with

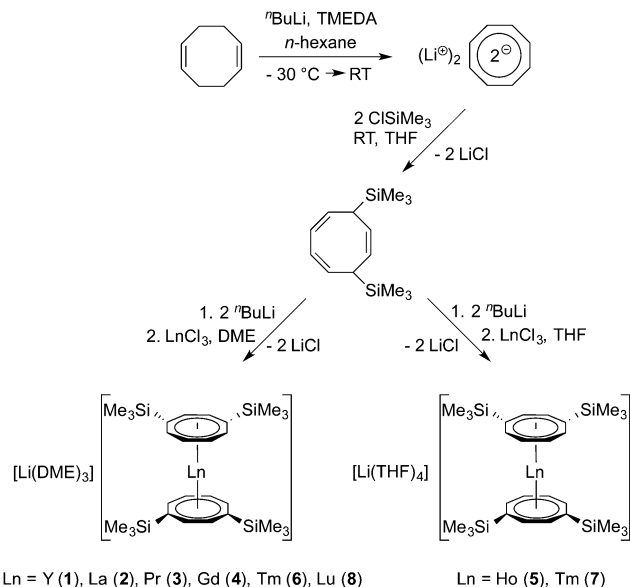
Ln = Y,¹⁹ Ce,¹⁹ Pr,¹⁹ Nd,^{14,19} Sm,¹⁹ Gd¹⁷ and Dy¹⁷ as well as the DME adducts [Li(DME)₃][Ln(COT^{''})₂] (Ln = Ce,^{14,20} Dy,¹⁷ Er²¹), Li(DME)Tb(COT^{''})₂²² and Li(THF)(DME)Dy(COT^{''})₂.²³ A notable neutral lanthanide sandwich complex containing COT^{''} is the cerocene derivative Ce(COT^{''})₂.²⁴ Sterically even more demanding is the 1,3,6-tris(trimethylsilyl)cyclooctatetraenyl dianion ligand (=COT^{'''}), which has also been successfully employed in organolanthanide^{24–26} and -actinide chemistry.^{24,27}

Recent findings by Murugesu and co-workers revealed that some of the anionic [Ln(COT^{''})₂][−] sandwich complexes behave as organometallic single-molecule magnets.^{17,20,21,23} Due to the renewed interest in this class of compounds, we carried out a broader investigation on lanthanide and actinide COT^{''} sandwich complexes. In this contribution we report the synthesis and structural characterization of the new anionic lanthanide sandwich complexes [Li(DME)₃][Ln(COT^{''})₂] (Ln = Y (**1**), La (**2**), Gd (**4**), Tm (**6**), Lu (**8**)) and [Li(THF)₄][Ln(COT^{''})₂] (Ln = Pr (**3**), Ho (**5**), Tm (**7**)) as well as the neutral actinide sandwich complexes An(COT^{''})₂ (An = Th (**9**), U (**10**)) and An(COT^{'''})₂ (An = Th (**11**), U (**12**)). Most recently, after this work had been completed, Murugesu *et al.* reported the synthesis, structure, and magnetic properties of the closely related uranium(III) sandwich complex [Li(DME)₃][U(COT^{''})₂] and the isostructural and isoelectronic lanthanide analogue [Li(DME)₃][Nd(COT^{''})₂]. This work also included the synthesis and structural characterization of the neutral uranocene derivative U(COT^{''})₂ (**10**), although its preparation involved a different synthetic route (*vide infra*).²⁷

2. Results and discussion

The general synthetic protocol for preparing the anionic lanthanide sandwich complexes is outlined in Scheme 3. The synthesis starts with the well-established preparation of 1,4-bis(trimethylsilyl)cycloocta-2,5,7-triene from 1,5-cyclooctadiene according to Cloke *et al.*¹⁰ The dilithium reagent Li₂COT^{''} can be conveniently prepared by metalation of 1,4-bis(trimethylsilyl)cycloocta-2,5,7-triene with *n*-butyllithium,¹⁰ and the resulting solutions can be used *in situ* for further reactions. However, it is also possible to isolate crystalline adducts of Li₂COT^{''}, *e.g.* [Li(TMEDA)]₂(COT^{''}) (TMEDA = *N,N,N',N'*-tetramethylethylenediamine),^{10c} [Li(DME)]₂(COT^{''}),^{28a} and [Li(THF)₂]₂[Li₂(COT^{''})₂].^{28b} The latter two adducts have been structurally characterized through X-ray diffraction. [Li(TMEDA)]₂(COT^{''}) was shown to be an inverse sandwich complex with the two Li⁺ ions coordinated to the bridging 1,4-bis(trimethylsilyl)cyclooctatetraene dianion ring in an η³-allyl-like fashion.^{28a} [Li(THF)₂]₂[Li₂(COT^{''})₂] contains two Li⁺ ions sandwiched between two COT^{''} rings and two Li(THF)₂⁺ units attached to the outside of the COT^{''} rings.^{28b} In the present study, however, it was found to be more convenient to use *in situ*-prepared THF solutions of Li₂COT^{''} rather than isolated samples. Accordingly, the anionic lanthanide sandwich complexes **1–8** were prepared by treatment of selected anhydrous lanthanide trichlorides, LnCl₃, with 2 equiv. of Li₂COT^{''} in THF solution as outlined in Scheme 3. In the case of the THF adducts [Li(THF)₄][Ln(COT^{''})₂] (Ln = Ho (**5**), Tm (**7**)),





Scheme 3 Synthetic route to the anionic lanthanide sandwich complexes **1–8**.

purification was achieved by recrystallization of the crude products from toluene. The DME adducts $[\text{Li}(\text{DME})_3][\text{Ln}(\text{COT}'')_2]$ ($\text{Ln} = \text{Y}$ (**1**), La (**2**), Pr (**3**), Gd (**4**), Tm (**6**), Lu (**8**)) were obtained by extraction of the reaction products with toluene followed by recrystallization from DME after addition of *n*-pentane. The products were isolated in moderate to good yields (57–75%) in the form of yellow or yellow-green (Tm: red), highly air-sensitive crystalline solids. It has been noted earlier that DME is the solvent of choice for crystallizing these anionic lanthanide sandwich complexes.^{14,20} The DME solvates are readily crystallized and the resulting crystals do not lose DME even under vacuum or upon prolonged storage in the dry-box. In contrast, crystals of the THF adducts are less stable with respect to loss of solvent and become opaque upon storing in the dry-box.

Meaningful NMR spectra could be obtained only for the diamagnetic products $[\text{Li}(\text{DME})_3][\text{Y}(\text{COT}'')_2]$ (**1**), $[\text{Li}(\text{DME})_3][\text{La}(\text{COT}'')_2]$

(**2**), and $[\text{Li}(\text{DME})_3][\text{Lu}(\text{COT}'')_2]$ (**8**) as well as for the paramagnetic praseodymium derivative **3**. In all four cases the ^1H and ^{13}C NMR data were in good agreement with the formation of the expected anionic sandwich complexes. The observation of only one signal in the ^{29}Si NMR spectra (**1**: 0.7 ppm, **2**: 0.5 ppm, **3**: –46 ppm, **8**: 0.8 ppm) indicated high purity of the materials. Moreover, the IR spectra of the DME adducts on one hand and the THF adducts on the other hand were found to be almost superimposable. All the new complexes were structurally characterized through single-crystal X-ray crystallography. Crystallographic data for **1–8** are summarized in Tables 1 and 2. The most significant bond lengths and angles are listed in Table 3.

All eight lanthanide complexes were found to form large crystals quite readily. X-ray quality single-crystals of the DME solvates $[\text{Li}(\text{DME})_3][\text{Ln}(\text{COT}'')_2]$ ($\text{Ln} = \text{Y}$ (**1**), La (**2**), Pr (**3**), Gd (**4**), Tm (**6**), Lu (**8**)) were obtained by recrystallization from solvent mixtures of DME and *n*-pentane (1 : 1) at room temperature. Single-crystals of the THF adducts $[\text{Li}(\text{THF})_4][\text{Ln}(\text{COT}'')_2]$ ($\text{Ln} = \text{Ho}$ (**5**), Tm (**7**)) were grown from concentrated solutions in THF at r.t. The molecular structure of the THF adduct $[\text{Li}(\text{THF})_4][\text{Ho}(\text{COT}'')_2]$ (**5**) is shown in Fig. 1, and Fig. 2 shows the molecular structure of $[\text{Li}(\text{DME})_3][\text{Lu}(\text{COT}'')_2]$ (**8**) as a representative DME adduct.

As can be seen from Table 3, the average Ln–C bond lengths vary between 2.785 Å in the lanthanum complex **2** and 2.609 Å in the lutetium derivative **8**. The difference of 0.176 Å can be attributed to the lanthanide contraction. Certainly the most significant result is the finding that all known $[\text{Li}(\text{DME})_3][\text{Ln}(\text{COT}'')_2]$ complexes ($\text{Ln} = \text{Y}$ (**1**), La (**2**), Ce ,^{14,20} Pr (**3**), Nd ,²⁷ Gd (**4**), Dy ,¹⁷ Er ,²¹ Tm (**6**), Lu (**8**)) and also the recently reported $[\text{Li}(\text{DME})_3][\text{U}(\text{COT}'')_2]$ ²⁷ crystallize in the triclinic space group $P\bar{1}$ and are isostructural. The same can be said about the series of known $[\text{Li}(\text{THF})_4][\text{Ln}(\text{COT}'')_2]$ complexes,^{14,17,19} including the new derivatives $[\text{Li}(\text{THF})_4][\text{Ho}(\text{COT}'')_2]$ (**5**) and (**b**) $[\text{Li}(\text{THF})_4][\text{Tm}(\text{COT}'')_2]$ (**7**). The *Ctr*–Ln–*Ctr* angles (*Ctr* = ring centroid) are found to be in the very narrow range between 177.8° for $[\text{Li}(\text{THF})_4][\text{Tm}(\text{COT}'')_2]$ (**7**) and 175.59° for

Table 1 Crystallographic data for **1–6**

	1	2	3	4	5	6
Empirical formula	$\text{C}_{40}\text{H}_{78}\text{LiO}_6\text{Si}_4\text{Y}$	$\text{C}_{40}\text{H}_{78}\text{LaLiO}_6\text{Si}_4$	$\text{C}_{40}\text{H}_{78}\text{LiO}_6\text{PrSi}_4$	$\text{C}_{40}\text{H}_{78}\text{GdLiO}_6\text{Si}_4$	$\text{C}_{44}\text{H}_{30}\text{HoLiO}_6\text{Si}_4$	$\text{C}_{40}\text{H}_{78}\text{LiO}_6\text{Si}_4\text{Tm}$
<i>a</i> (Å)	11.445(2)	11.557(2)	11.532(2)	11.428(2)	11.358(2)	11.410(2)
<i>b</i> (Å)	12.219(2)	12.262(3)	12.286(3)	12.216(2)	12.657(2)	12.239(2)
<i>c</i> (Å)	18.477(4)	18.340(4)	18.388(4)	18.406(4)	19.603(4)	18.503(4)
α (°)	99.13(3)	98.83(3)	98.82(3)	98.84(3)	87.12(3)	99.12(3)
β (°)	102.20(3)	102.56(3)	102.49(3)	102.36(3)	82.38(3)	102.17(3)
γ (°)	99.68(3)	98.57(3)	99.04(3)	99.44(3)	77.39(3)	100.11(3)
<i>V</i> (Å ³)	2438.7(8)	2461.6(9)	2464.1(9)	2428.0(8)	2509.9(9)	2434.9(8)
<i>Z</i>	2	2	2	2	2	2
Formula weight	863.23	913.23	915.23	931.57	957.31	943.25
Space group	$P\bar{1}$	$P\bar{1}$	$P\bar{1}$	$P\bar{1}$	$P\bar{1}$	$P\bar{1}$
<i>T</i> (K)	153(2)	133(2)	153(2)	133(2)	153(2)	153(2)
λ (Å)	0.71073	0.71073	0.71073	0.71073	0.71073	0.71073
<i>D</i> _{calc} (g cm ^{−3})	1.176	1.232	1.234	1.274	1.267	1.287
μ (mm ^{−1})	1.332	1.003	1.124	1.503	1.707	1.959
<i>R</i> (<i>F</i> _o or <i>F</i> _o ²)	0.0467	0.0381	0.0267	0.0333	0.0491	0.0319
<i>R</i> _w (<i>F</i> _o or <i>F</i> _o ²)	0.1018	0.0944	0.0662	0.0883	0.0859	0.0771

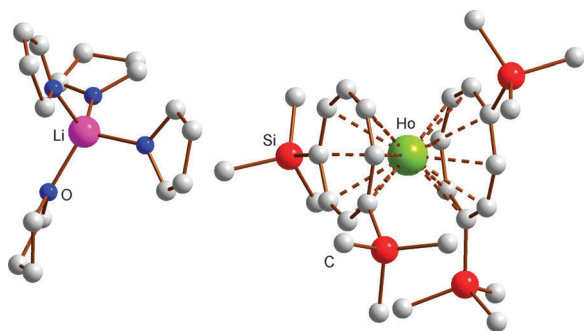
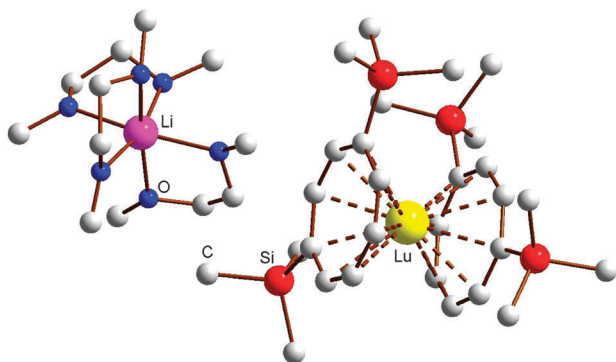


Table 2 Crystallographic data for 7–12

	7	8	9	10	11	12
Empirical formula	C ₄₄ H ₈₀ LiO ₄ Si ₄ Tm	C ₄₀ H ₇₈ LiLuO ₆ Si ₄	C ₂₈ H ₄₈ Si ₄ Th	C ₂₈ H ₄₈ Si ₄ U	C ₃₄ H ₆₄ Si ₆ Th	C ₃₄ H ₆₄ Si ₆ U
<i>a</i> (Å)	11.358(2)	11.471(2)	9.830(3)	12.6598(12)	20.9990(12)	23.381(3)
<i>b</i> (Å)	11.657(2)	12.051(2)	9.898(3)	20.3542(18)	25.1674(15)	21.170(3)
<i>c</i> (Å)	19.603(4)	18.459(4)	17.038(5)	24.645(2)	17.8458(10)	18.125(2)
α (°)	87.12(3)	99.79(3)	79.262(4)	90	90	90
β (°)	82.38(3)	101.72(3)	80.692(4)	90	114.3160(10)	107.923(2)
γ (°)	77.39(3)	100.05(3)	80.891(3)	90	90	90
<i>V</i> (Å ³)	2509.9(9)	2403.6(8)	1.5932(8)	6350.6(10)	8594.7(9)	8536.3(18)
<i>Z</i>	2	2	2	8	8	8
Formula weight	961.31	949.29	729.06	735.05	873.43	879.42
Space group	<i>P</i> $\bar{1}$	<i>P</i> $\bar{1}$	<i>P</i> $\bar{1}$	<i>Pbca</i>	<i>C2/c</i>	<i>P2₁/c</i>
<i>T</i> (K)	153(2)	143(2)	100(2)	173(2)	200(2)	200(2)
λ (Å)	0.71073	0.71073	0.71073	0.71073	0.71073	0.71073
<i>D</i> _{calcd} (g cm ⁻³)	1.272	1.312	1.520	1.538	1.350	1.369
μ (mm ⁻¹)	1.899	2.192	4.845	5.277	3.657	3.991
<i>R</i> (<i>F</i> _o or <i>F</i> _o ²)	0.0390	0.0557	0.0472	0.0238	0.0301	0.0421
<i>R</i> _w (<i>F</i> _o or <i>F</i> _o ²)	0.1015	0.1473	0.1084	0.0838	0.0675	0.1127

Table 3 Selected average bond lengths (Å) and angles (°) of the lanthanide sandwich complexes 1–8. *Ctr* stands for the COT'' ring centroids

	Y (1)	La (2)	Pr (3)	Gd (4)	Ho (5)	Tm (6)	Tm (7)	Lu (8)
Ln–C	2.649	2.785	2.740	2.680	2.607	2.624	2.615	2.609
C–C	1.413	1.414	1.414	1.416	1.414	1.417	1.414	1.412
Si–C	1.865	1.867	1.866	1.867	1.868	1.867	1.868	1.864
Li–O	2.135	2.133	2.134	2.134	1.921	2.135	1.919	2.123
Ln– <i>Ctr</i>	1.900	2.084	2.020	1.940	1.873	1.861	1.850	1.845
<i>Ctr</i> –Ln– <i>Ctr</i>	176.19	175.59	175.80	175.74	177.6	176.6	177.8	176.86

Fig. 1 Molecular structure of [Li(THF)₄][Ho(COT'')₂] (5).Fig. 2 Molecular structure of [Li(DME)₃][Lu(COT'')₂] (8).

[Li(DME)₃][Ln(COT'')₂] (2). Thus there is only little deviation from the ideal linear sandwich arrangement. Clearly, the bulky cyclooctatetraenyl ligand COT'' is ideally suited for studying homologous series of lanthanide and actinide sandwich complexes comprising the full range of ionic radii possible. Table 4 provides an overview of all anionic lanthanide sandwich complexes of the types [Li(THF)₄][Ln(COT'')₂] and [Li(DME)₃][Ln(COT'')₂] reported thus far in order to show which gaps have been filled by the present study.

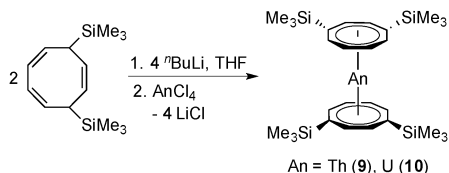
In a similar manner, the closely related neutral actinidocenes An(COT'')₂ (An = Th (9), U (10)) have also been prepared. As outlined in Scheme 4, these sandwich complexes were prepared in a straightforward manner by reaction of anhydrous ThCl₄ or UCl₄ with 2 equiv. of *in situ*-prepared Li₂COT''. Due to the high solubility of all the reactants in THF, the reactions were finished after 2 h stirring at r.t. In contrast, reactions of AnCl₄ with the unsubstituted K₂COT normally take days.^{11,12} Bright yellow Th(COT'')₂ (9) and dark green (dichroic red/green) U(COT'')₂ (10) were both isolated in high yields of ca. 80%. Purification could be achieved either by high-vacuum sublimation at 240 °C or by slow crystallization from the oily crude products. In this context it is interesting to note that Murugesu *et al.* very recently prepared compound 10 *via* a two-step synthesis where U^{III}I₃(1,4-dioxane)_{1.5} and [Li(THF)₂]₂[Li₂(COT'')₂]₂^{28b} were first combined in THF to afford the anionic uranium(III) sandwich complex [Li(DME)₃][U(COT'')₂] which was then oxidized to the uranium(IV) sandwich 10 using FeCl₂.²⁷

For comparison, two neutral actinide sandwich complexes comprising the bulky 1,3,6-tris(trimethylsilyl)cyclooctatetraenyl ligand (COT''') have also been prepared. These compounds have earlier been mentioned in two communications, but structural characterization through X-ray diffraction was lacking.²⁴ Both compounds were prepared according to the straightforward synthetic protocol illustrated in Scheme 5. In this case, the use of the potassium precursor K₂COT''' provided products 11 and 12 in yields of around 80% after crystallization from concentrated solutions in *n*-pentane. Like their tetrasubstituted

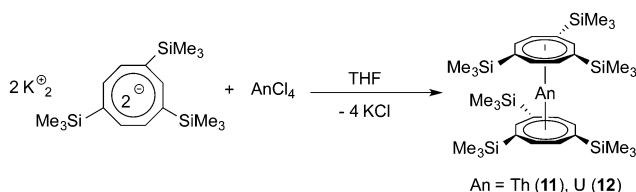


Table 4 Overview of all known anionic lanthanide sandwich complexes of the type $[\text{Li}(\text{THF})_4][\text{Ln}(\text{COT}'')_2]$ (denoted THF) and $[\text{Li}(\text{DME})_3][\text{Ln}(\text{COT}'')_2]$ (denoted DME). X: compounds described in this work

Ln	Y	La	Ce	Pr	Nd	Sm	Eu	Gd	Tb	Dy	Ho	Er	Tm	Yb	Lu
THF	X ¹⁹		X ¹⁹	X ¹⁹	X ^{14,19}	X ¹⁹		X ¹⁷		X ¹⁷	X		X		
DME	X	X	X ^{14,20}	X				X		X ¹⁷		X ²¹	X		X



Scheme 4 Synthetic route to the neutral actinidocenes $\text{An}(\text{COT}'')_2$ ($\text{An} = \text{Th}$ (**9**), U (**10**)).



Scheme 5 Synthesis of the neutral actinidocenes $\text{An}(\text{COT}''')_2$ ($\text{An} = \text{Th}$ (**11**), U (**12**)).

congeners **9** and **10**, thorium compound **11** forms bright yellow crystals, while crystals of **12** appear dichroitic red/green. Both complexes are highly soluble in common organic solvents, including hydrocarbons.

All four silyl-substituted actinidocenes **9–12** have been structurally characterized through single-crystal X-ray diffraction. Crystallographic data for **9–12** are summarized in Table 2; selected bond lengths and angles are listed in Table 4. The molecular structures are depicted in Fig. 3 and 4. As can be seen from the structural data listed in Table 4, the overall structural features of all four actinidocene derivatives studied here are very similar. According to the unsymmetrical substitution pattern on the cyclooctatetraenyl rings leading to steric interactions, all complexes show a slight distortion from the ideal linear arrangement with *Ctr*–*M*–*Ctr* angles of about 174°. As expected, evidence for actinide contraction is found which is

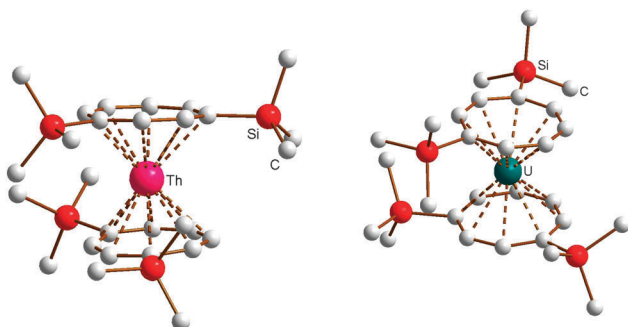


Fig. 3 Molecular structures of $\text{Th}(\text{COT}'')_2$ (**9**) and $\text{U}(\text{COT}'')_2$ (**10**).

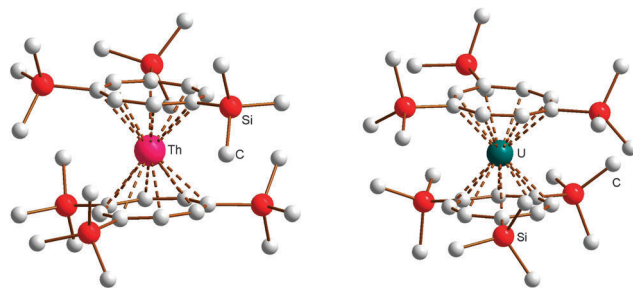


Fig. 4 Molecular structures of $\text{Th}(\text{COT}''')_2$ (**11**) and $\text{U}(\text{COT}''')_2$ (**12**).

Table 5 Selected average bond lengths (Å) and angles (°) of the actinide sandwich complexes **9–12**. *Ctr* stands for the COT ring centroids; mean values are given in parentheses

	Th (9)	U (10)	Th (11)	U (12)
M–C	2.696–2.745 (2.718)	2.642–2.69.0 (2.663)	2.709–2.763 2.705–2.762 (2.735/2.732)	2.643–2.727 2.647–2.727 (2.679/2.681)
M– <i>Ctr</i>	1.987 1.999 (1.993)	1.921/1.913 (1.917)	2.012 2.010 (2.011)	1.942, 1.944 1.938, 1.945 (1.942)
<i>Ctr</i> –M– <i>Ctr</i>	172.9	173.0	174.3, 175.3	174.3, 174.9
<i>Pl</i> // <i>Pl</i>	7.1	7.4	6.3	5.7/6.0

reflected in ~5 pm shorter M–C as well as in ~7 pm shorter M–*Ctr* distances in the uranium complexes as compared to the thorium species (Table 5).

In the following, the structural and spectroscopic characterization of **10** as a typical example will be discussed in more detail. The molecular structure of **10** can be clearly described as being of the well-known uranocene type (Fig. 5). Accordingly, in the molecular structure the central uranium atom is placed between the two cyclooctatetraenyl rings with U–*Ctr* distances of 1.913 or 1.921 Å, comparable to previously reported uranocene derivatives²⁹ (Table 4). However, the trimethylsilyl substituents in 1,4-positions of the cyclooctatetraenyl ring lead to an arrangement in the solid state where on one side of the molecule a stronger steric interaction between the two cyclooctatetraenyl rings results. Si1 and Si4 are found to be in closer steric environment than Si2 and Si3, giving rise to a significant repulsion on this side of the rings. This has an influence on the bond lengths and angles in that the two cyclooctatetraenyl rings do not bind symmetrically to the central uranium atom. The U–C bond distances cover a range between 2.642 and 2.690(4) Å with the longer bond lengths found on the side with the stronger steric interactions, whereas the shortest U–C bond length is observed for U1–C22 with 2.642(4) Å. Accordingly, the two cyclooctatetraenyl rings are not coordinated coplanar with



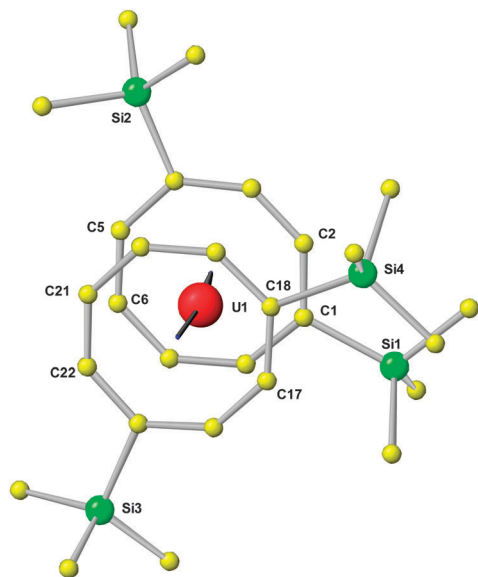


Fig. 5 Top view of the molecular structure of $U(COT'')_2$ (**10**).

respect to the uranium center. This results in a *Ctr*–*U*–*Ctr* angle of 7.0° and a tilt angle between the two ring planes of 7.4° with the opening to the side of Si1/Si4 (Table 4 and Fig. 5). This is further reflected in the corresponding distances between opposing carbon atoms of the two COT'' rings in the staggered structure. With 4.047 and 4.070 Å the distances C1–C17 and C2–C18 are remarkably longer than those between C5 and C21 or C6 and C22, which are with 3.627 or 3.614 Å significantly shorter. These structural findings clearly show that compound **10** shows typical uranocene structural features^{29a} but with a significant distortion caused by steric effects due to the trimethylsilyl substituents at the COT rings. A significantly stronger tilting of the two cyclooctatetraenyl rings has been observed in the 1,4-bis(trimethylsilyl)-substituted system where ring-to-ring C–C distances between 3.468 and 4.247 Å and a tilt angle of 11.4° have been found.³⁰

The spectroscopic data of the complexes **9–12** are in good agreement with their structural features. As expected, the IR spectra of **9–12** are all very similar, showing the comparable molecular constitution of these actinidocenes. Frequencies arising from the COT'' ligand increase slightly upon complexation as compared to K_2COT'' . However, the spectra are more complicated than those of the unsubstituted actinidocenes as the $SiMe_3$ -substituents give rise to strong absorptions themselves and cause a distortion from the ideal D_{8h} -symmetry observed in the actinidocenes, leading to a higher number of observed frequencies.³¹ However, the general congruency of the IR and FIR spectra clearly shows the similarity in the structural features of the complexes **9–12**. The other spectroscopic data will be highlighted taking again compound **10** as example. In contrast to the corresponding Th-complex **9**, the uranocene derivative **10** exhibits a $5f^2$ -electron configuration causing paramagnetism and an intensely red color in transmission. These findings are confirmed by the UV-vis data (Fig. 6), showing that below 450 nm the absorption of the complex is strongly increasing.

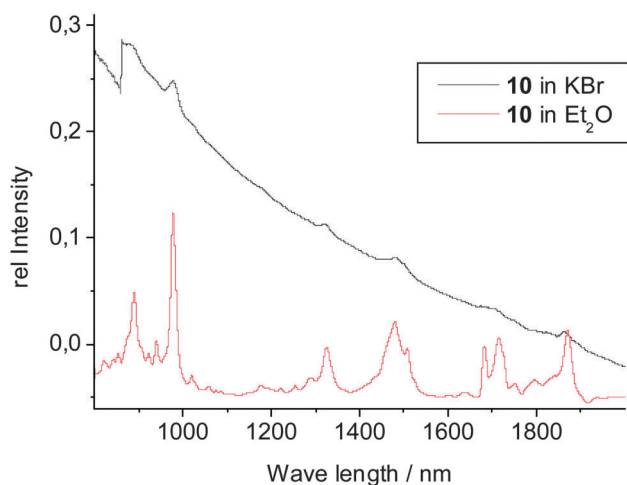
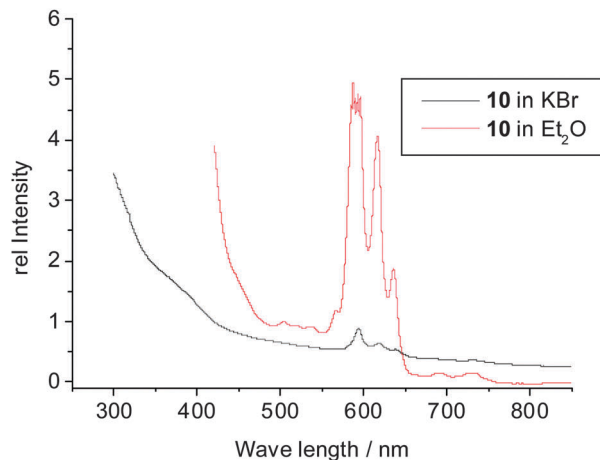


Fig. 6 UV-vis spectra of $U(COT'')_2$ (**10**).

The absorptions at 592, 618, 635 nm are caused by strong charge transfer transitions typical for actinocene complexes, however being more intense in symmetry-distorted systems.³² In the range of 800 to 2000 nm, the UV-vis spectrum does not show any significant differences between the solid state and the solution, indicating that the solid state structure is retained in solution and no adduct formation takes place. Accordingly, the absorptions at 980, 1322, 1486, 1710, 1755, 1793, 1865 nm are caused by f–f transitions, which are characteristic of $U(IV)$ -organometallics.³³ The f–f transitions are in this case of higher intensity than for the unsubstituted uranocene due to the observed distortion of the complex symmetry by the $SiMe_3$ substituents, which causes an increase in the intensity for the symmetry-forbidden f–f transitions. These are, however, between 10 to 100 times less intense than the charge transfer absorptions.

The paramagnetism of **10** is also clearly seen from its NMR data (Fig. 7–9), where for all signals a typical upfield shift is observed.^{7a,34} In good agreement with the solid state structure, the 1H NMR spectrum of **10** (Fig. 7) shows four well-separated singlets at -9.99 , -25.20 , -39.63 , and -45.62 ppm. The latter three each correspond to four ring protons, whereas the first



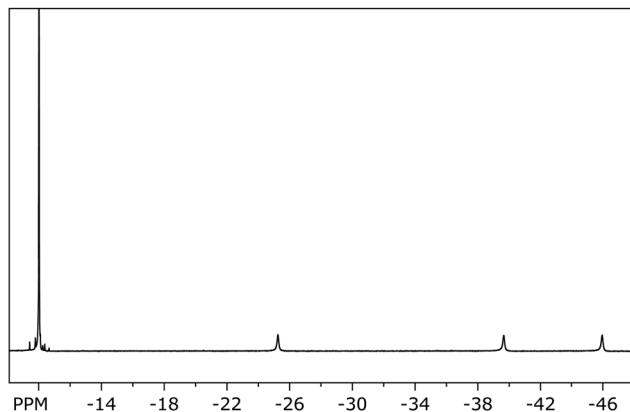


Fig. 7 ^1H NMR spectrum of $\text{U}(\text{COT}'')_2$ (**10**).

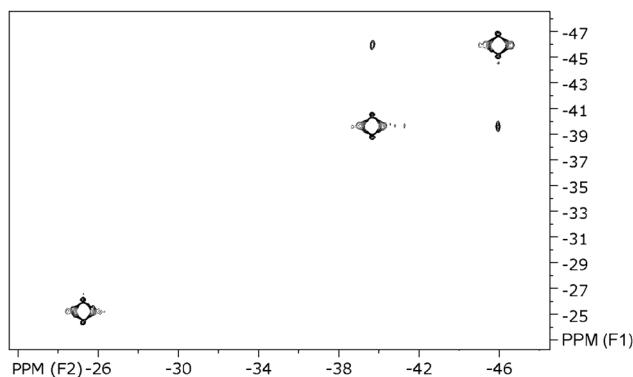


Fig. 8 HH correlated NMR spectrum of $\text{U}(\text{COT}'')_2$ (**10**).

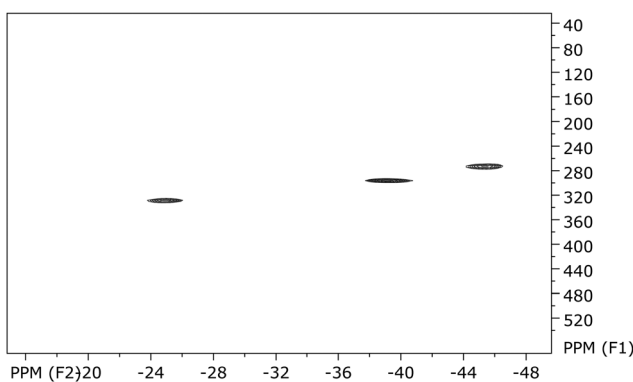


Fig. 9 CH correlated NMR spectrum of $\text{U}(\text{COT}'')_2$ (**10**).

resonance can be clearly assigned to the protons of the SiMe_3 substituents. In the two-dimensional HH-correlated spectrum the resonances at -39.63 and -45.62 ppm (β -position to the SiMe_3 -substituents) are assigned to the protons in the $(\text{CH})_4$ -chain of the COT'' ring, whereas the resonance at -25.20 ppm corresponds to the ring protons positioned between the two trimethylsilyl substituents in 1,4-positions (Fig. 8).

This assignment is in good agreement with the published data where a strong influence of the paramagnetism on the chemical shifts in uranocene derivatives is described.³⁴

However, in this paper, for the first time, the ^{13}C chemical shifts of a uranocene complex are reported. The carbon resonance of the SiMe_3 groups was localized at -3.5 ppm. The proton resonance at -25.20 ppm exhibits a cross peak at 325.9 ppm in the ^{13}C frequency, whereas the two coupling H-atoms of the aromatic ring at -39.63 ppm and -45.62 ppm give rise to carbon resonances as well at low field shifts with 293.8 and 270.3 ppm, respectively (Fig. 9). The observation of carbon frequencies at these low fields is in agreement with theoretical predictions.³⁵

3. Conclusions

In summarizing the results reported here, the series of anionic lanthanide(III) sandwich complexes of the type $[\text{Ln}(\text{COT}'')_2]^-$ ($\text{COT}'' = 1,4$ -bis(trimethylsilyl)cyclooctatetraenyl dianion) has been largely extended through the synthesis of eight new derivatives ranging from lanthanum to lutetium. Surprisingly, neither the ionic radius nor the oxidation state of the f-element ion ($\text{Ln}^{3+}/\text{An}^{4+}$) have a pronounced influence on the structural features of the compounds $[\text{Li}(\text{DME})_3][\text{Ln}(\text{COT}'')_2]$ (**1–8**; $\text{Ln} = \text{Y}, \text{La}, \text{Pr}, \text{Gd}, \text{Tm}, \text{Lu}$), $[\text{Li}(\text{THF})_4][\text{Ln}(\text{COT}'')_2]$ (**5, 7**; $\text{Ln} = \text{Ho}, \text{Tm}$), $\text{An}(\text{COT}'')_2$ (**9, 10**; $\text{An} = \text{Th}, \text{U}$) and $\text{An}(\text{COT}''')_2$ (**11, 12**; $\text{An} = \text{Th}, \text{U}$). In all cases the slight deviation from the ideal sandwich structure is in the same range. Through this comparative study anionic sandwich complexes containing the $[\text{Ln}(\text{COT}'')_2]^-$ anions have now become available for the entire series of rare-earth metals. This should allow for more detailed investigations *e.g.* of the magnetic properties in the course of future studies.

4. Experimental section

4.1 General procedures

All operations were performed with rigorous exclusion of air and water in oven-dried or flame-dried glassware under an inert atmosphere of dry argon, employing standard Schlenk, high-vacuum and glovebox techniques (MBraun MBLab; <1 ppm O_2 , <1 ppm H_2O). THF, DME, toluene, and cyclopentane were dried over sodium/benzophenone and freshly distilled under a nitrogen atmosphere prior to use. All glassware was oven-dried at 120 °C for at least 24 h, assembled while hot, and cooled under high vacuum, prior to use. The starting materials, anhydrous LnCl_3 ($\text{Ln} = \text{Ce}, \text{Nd}$),³⁶ ThCl_4 ,³⁷ UCl_4 ,³⁸ $\text{C}_8\text{H}_8(\text{SiMe}_3)_2$,¹⁰ $\text{Li}_2(\text{COT}'')$,¹⁰ and $\text{K}_2\text{COT}''''$ ^{24,25} were prepared according to the published procedures. The NMR spectra were recorded in C_6D_6 or d_8 -THF solutions on a Bruker AVANCE 600 (^1H : 600.1 MHz; ^{13}C : 150.9 MHz) or a Bruker AVANCE 400 (5 mm BB, ^1H : 400.1 MHz; ^{13}C : 100.6 MHz) (Ln compounds), or a Bruker-AVANCE 250 (5 mm TBI, ^1H : 250.1 MHz; ^{13}C : 62.5 MHz) (An compounds). ^1H and ^{13}C shifts are referenced to internal solvent resonances and reported in parts per million relative to TMS. IR (KBr) spectra were recorded using a Perkin-Elmer FT-IR 2000 spectrometer. UV-Vis spectra were registered on a Perkin-Elmer Lambda 2 spectrometer. Mass spectra (EI, 70 eV) were run on a MAT 95 apparatus. Microanalyses of the compounds were performed



using a Leco CHNS 932 apparatus. Metal analyses were performed *via* ICP AES.

4.2 Preparation of the anionic lanthanide sandwich complexes 1–8 (general synthetic protocols)

(a) DME solvates [Li(DME)₃][Ln{C₈H₆(SiMe₃)₂}₂] (Ln = Y (1), La (2), Pr (3), Gd (4), Tm (6), Lu (8)). Li₂(COT^{''}) was prepared *in situ* by adding 15.0 mL (24.0 mmol) of a 1.6 M *n*-butyllithium solution in *n*-hexane at r.t. to a solution of 3.0 g (12.0 mmol) C₈H₈(SiMe₃)₂ in 150 mL of THF. 6.0 mmol of anhydrous LnCl₃ were added as a solid, the reaction mixture was stirred for 24 h and the solvents were completely removed under vacuum. The solid residue was extracted with 150 mL of toluene. After filtration, the toluene was again completely removed under vacuum and replaced by 30 mL of DME. After addition of the same amount of *n*-pentane, the products [Li(DME)₃]-[Ln{C₈H₆(SiMe₃)₂}₂] crystallized upon standing at room temperature for a few days.

(b) THF solvates [Li(THF)₄][Ln{C₈H₆(SiMe₃)₂}₂] (Ln = Ho (5), Tm (7)). The reactions were carried out exactly in the same manner as described above. After extraction of the products with toluene and filtration, the volume of the solution was reduced to ~20 mL. The products [Li(THF)₄][Ln{C₈H₆(SiMe₃)₂}₂] crystallized directly upon standing at room temperature for a few days.

[Li(DME)₃][Y{C₈H₆(SiMe₃)₂}₂] (1). Yield: 3.57 g (69%), dec. > 90 °C. Elemental analysis calcd. for C₄₀H₇₈LiO₆Si₄Y (M_r = 863.24 g mol⁻¹): C, 55.66; H, 9.11. Found: C, 54.98; H, 8.88%. IR (KBr disc): ν = 3222m, 3092m, 3037m, 2962s, 2933s, 2531m, 2360m, 2224m, 2029m, 1959m, 1638vs, 1497m, 1445s, 1408s, 1384s, 1371s, 1309s, 1248vs, 1181s, 1155s, 1044m, 1027m, 985m, 934w, 837vs, 810m, 750m, 719m, 692w, 651w, 636w, 626w, 589vw, 555w, 505w, 480vw, 457vw cm⁻¹. ¹H NMR (400.1 MHz, *d*₈-THF, 24 °C): δ = 3.40 (s, 12H, DME), 3.26 (s, 18H, DME), 0.43 (s, 36H, Si(CH₃)₃), 6.09–6.04 (m, 8H, COT-*H*), 5.91–5.87 (m, 4H, COT-*H*) ppm. ¹³C NMR (100.6 MHz, *d*₈-THF, 24 °C): δ = 99.4 (COT), 99.3 (COT), 97.3 (COT), 96.6 (COT), 72.7 (DME), 58.9 (DME), 1.6 (Si(CH₃)₃) ppm. ²⁹Si NMR (79.5 MHz, *d*₈-THF, 24 °C): δ = 0.7 ppm. MS (EI): *m/z* 586 (26%, [C₈H₆(SiMe₃)₂Y]), 514 (6, [C₈H₆(SiMe₃)₂Y-SiMe₃]), 337 (35, [C₈H₆(SiMe₃)₂Y]), 263 (14, [C₈H₆(SiMe₃)₂Y-SiMe₃]), 248 (42, [C₈H₆(SiMe₃)₂]), 207 (66, [C₈H₆(SiMe₃)₂-3Me]).

[Li(DME)₃][La{C₈H₆(SiMe₃)₂}₂] (2). Yield: 3.34 g (61%), dec. 104 °C. Elemental analysis calcd. for C₄₀H₇₈LaLiO₆Si₄ (M_r = 913.25 g mol⁻¹): C, 52.61; H, 8.61. Found: C, 52.70; H, 8.10%. IR (KBr disc): ν = 3436w, 3223w, 3090w, 2995m, 2954s, 2897m, 2830w, 2537vw, 2363vw, 2100vw, 1959vw, 1868vw, 1757vw, 1638w, 1599w, 1452w, 1405w, 1370w, 1312w, 1248s, 1210w, 1193w, 1181w, 1156w, 1124w, 1086m, 1065w, 1052m, 1028w, 981w, 932w, 910w, 837vs, 783vs, 750m, 716m, 690w, 681w, 651w, 636w, 550vw, 514vw, 504vw, 478vw, 459vw, 423vw cm⁻¹. ¹H NMR (400.1 MHz, *d*₈-toluene, 24 °C): δ = 2.31 (s, 18H, DME), 1.94 (s, 12H, DME), 0.67 (s, 36H, Si(CH₃)₃), 6.51–6.44 (m, 8H, COT-*H*), 6.40–6.35 (m, 4H, COT-*H*) ppm. ¹³C NMR (100.6 MHz, *d*₈-toluene, 24 °C): δ = 103.6 (COT), 102.6 (COT), 101.3 (COT), 100.3 (COT), 69.3 (DME), 57.5 (DME), 1.1 (Si(CH₃)₃) ppm.

²⁹Si NMR (79.5 MHz, *d*₈-toluene, 24 °C): δ = 0.5 ppm. MS (EI): *m/z* 636 (1%, [C₈H₆(SiMe₃)₂La]), 387 (38, [C₈H₆(SiMe₃)₂La]), 248 (28, [C₈H₆(SiMe₃)₂]), 207 (34, [C₈H₆(SiMe₃)₂-3Me]).

[Li(DME)₃][Pr{C₈H₆(SiMe₃)₂}₂] (3). Yield: 4.12 g (75%), dec. 98 °C. Elemental analysis calcd. for C₄₀H₇₈LiO₆PrSi₄ (M_r = 915.25 g mol⁻¹): C, 52.49; H, 8.59. Found: C, 51.49; H, 8.31%. IR (KBr disc): ν = 3437m, 3222m, 3091m, 3036m, 2960s, 2933m, 2535w, 2224vw, 2029vw, 1972vw, 1959w, 1743vw, 1637s, 1447m, 1419m, 1383m, 1371m, 1343m, 1308s, 1245vs, 1181s, 1157vs, 1081m, 1050m, 985m, 933w, 909vw, 837s, 745m, 733w, 698w, 637w, 588vw, 555w, 504m, 467vw, 458vw, 451vw cm⁻¹. ¹H NMR (400.1 MHz, *d*₈-THF, 25 °C): δ = 3.63 (12H, DME), 3.31 (18H, DME), -6.17 (s, 27H, Si(CH₃)₃), -13.52, -9.54, -0.05 (br, s, COT-*H*) ppm. ¹³C NMR (100.6 MHz, *d*₈-THF, 25 °C): δ = 229.5 (COT), 216.6 (COT), 204.9 (COT), 192.7 (COT), 72.8 (DME), 59.0 (DME), 0.6 (Si(CH₃)₃) ppm. ²⁹Si NMR (79.5 MHz, *d*₈-THF, 25 °C): δ = -46 ppm. MS (EI): *m/z* 637 (4%, [C₈H₆(SiMe₃)₂Pr]), 389 (100, [C₈H₆(SiMe₃)₂Pr]), 315 (10, [C₈H₆(SiMe₃)₂Pr-SiMe₃]), 248 (22, [C₈H₆(SiMe₃)₂]), 207 (26, [C₈H₆(SiMe₃)₂-3Me]).

[Li(DME)₃][Gd{C₈H₆(SiMe₃)₂}₂] (4). Yield: 4.08 g (73%), dec. 128 °C. Elemental analysis calcd. for C₄₀H₇₈GdLiO₆Si₄ (M_r = 931.59 g mol⁻¹): C, 51.57; H, 8.44. Found: C, 50.83; H, 8.59%. IR (KBr disc): ν = 3788vw, 3546w, 3220w, 2997m, 2953s, 2897m, 2829m, 2540vw, 2101vw, 1959vw, 1871vw, 1800vw, 1753vw, 1637w, 1599w, 1543w, 1474w, 1451m, 1404w, 1369w, 1310w, 1248s, 1210w, 1192w, 1124m, 1086m, 1066m, 1053m, 1028w, 982w, 933m, 909w, 837vs, 782w, 769w, 750m, 717m, 680w, 651w, 636w, 548w, 521vw, 510w, 478vw, 459vw, 421vw cm⁻¹. NMR data could not be obtained for [Li(DME)₃]-[Gd{C₈H₆(SiMe₃)₂}₂] due to the paramagnetic character of the Gd³⁺-ion. MS (EI): *m/z* 655 (6%, [C₈H₆(SiMe₃)₂Gd]), 580 (1, [C₈H₆(SiMe₃)₂Gd-SiMe₃]), 406 (14, [C₈H₆(SiMe₃)₂Gd]), 335 (9, [C₈H₆(SiMe₃)₂Gd-SiMe₃]), 248 (54, [C₈H₆(SiMe₃)₂]), 207 (32, [C₈H₆(SiMe₃)₂-3Me]).

[Li(THF)₄][Ho{C₈H₆(SiMe₃)₂}₂] (5). Yield: 3.30 g (57%), dec. 113 °C. Elemental analysis calcd. for C₄₄H₈₀LiO₄Si₄Ho (M_r = 957.33 g mol⁻¹): C, 55.20; H, 8.42. Found: C, 54.93; H, 8.29%. IR (KBr disc): ν = 3036w, 2953vs, 2896s, 2833m, 2088vw, 1932vw, 1876vw, 1834vw, 1779vw, 1667vw, 1590w, 1536w, 1487w, 1446m, 1403m, 1317w, 1247vs, 1214m, 1049s, 1038m, 982m, 939s, 910m, 894m, 839vs, 783m, 748s, 735vs, 686m, 651w, 636s, 573vw, 550m, 540w, 522vw, 512w, 488vw, 463vw, 423vw cm⁻¹. NMR data could not be obtained for [Li(THF)₄]-[Ho{C₈H₆(SiMe₃)₂}₂] due to the paramagnetic character of the Ho³⁺-ion. MS (EI): *m/z* 662 (5%, [C₈H₆(SiMe₃)₂Ho]), 589 (5, [C₈H₆(SiMe₃)₂Ho-SiMe₃]), 412 (5, [C₈H₆(SiMe₃)₂Ho]), 340 (30, [C₈H₆(SiMe₃)₂Ho-SiMe₃]), 248 (40, [C₈H₆(SiMe₃)₂]), 206 (100, [C₈H₆(SiMe₃)₂-3Me]).

[Li(DME)₃][Tm{C₈H₆(SiMe₃)₂}₂] (6). Yield: 3.79 g (67%), dec. 125 °C. Elemental analysis calcd. for C₄₀H₇₈LiO₆Si₄Tm (M_r = 943.27 g mol⁻¹): C, 50.93; H, 8.33. Found: C, 50.50; H, 7.95%. IR (KBr disc): ν = 3469w, 3222w, 2994m, 2956s, 2898m, 2535vw, 1959vw, 1637m, 1450w, 1406w, 1385w, 1314w, 1248s, 1212w, 1181w, 1152w, 1125w, 1081w, 1052w, 1028w, 982w, 934w, 837vs, 750m, 736w, 719m, 691w, 651w, 634w, 547vw, 519vw, 505vw, 479vw, 463vw cm⁻¹. NMR data could not be obtained for



[Li(DME)₃][Tm{C₈H₆(SiMe₃)₂}₂] due to the paramagnetic character of the Tm³⁺-ion.

[Li(THF)₄][Tm{C₈H₆(SiMe₃)₂}₂] (7). Yield: 3.17 g (55%), dec. 133 °C. Elemental analysis calcd. for C₄₄H₈₀LiO₄Si₄Tm (*M_r* = 961.33 g mol⁻¹): C, 54.97; H, 8.39. Found: C, 54.15; H, 7.80%. IR (KBr disc): ν = 3469vw, 3030m, 2996m, 2952s, 2897m, 2830m, 2543vw, 2349vw, 2271vw, 2102vw, 1959vw, 1872vw, 1803vw, 1754vw, 1636w, 1599w, 1549w, 1475ww, 1451m, 1404w, 1369w, 1328w, 1311w, 1247s, 1214w, 1192w, 1158w, 1124m, 1087s, 1053m, 1028w, 983w, 934m, 911w, 836vs, 783w, 771w, 750m, 719s, 680w, 651w, 636m, 573vw, 547w, 518vw, 507w, 479vw, 457vw, 423vw cm⁻¹. NMR data could not be obtained for [Li(DME)₃][Tm{C₈H₆(SiMe₃)₂}₂] due to the paramagnetic character of the Tm³⁺-ion. MS (EI): *m/z* 665 (8%, [C₈H₆(SiMe₃)₂Tm]), 593 (2, [C₈H₆(SiMe₃)₂Tm-SiMe₃]), 417 (22, [C₈H₆(SiMe₃)₂Tm]), 343 (3, [C₈H₆(SiMe₃)₂Tm-SiMe₃]), 248 (48, [C₈H₆(SiMe₃)₂]), 207 (66, [C₈H₆(SiMe₃)₂-3Me]).

[Li(DME)₃][Lu{C₈H₆(SiMe₃)₂}₂] (8). Yield: 4.21 g (74%), dec. ca. 90 °C. Elemental analysis calcd. for C₄₀H₇₈LiLuO₆Si₄ (*M_r* = 949.31 g mol⁻¹): C, 50.61; H, 8.28. Found: C, 49.47; H, 8.20%. IR (KBr disc): ν = 3437w, 3222w, 2994m, 2956s, 2897m, 2536vw, 2354vw, 2096vw, 1959vw, 1868vw, 1635w, 1599m, 1452w, 1406w, 1385w, 1317w, 1248s, 1206w, 1181w, 1113w, 1097w, 1065w, 1044w, 1028w, 983w, 940w, 837vs, 810m, 750m, 738w, 720m, 692w, 674w, 651w, 624w, 556vw, 503vw, 478vw, 459w, 437vw, 422vw cm⁻¹. ¹H NMR (400.1 MHz, *d*₈-THF, 25 °C): δ = 3.39 (s, 12H, DME), 3.25 (s, 18H, DME), 0.43 (s, 36H, Si(CH₃)₃), 6.06–6.03 (m, 8H, COT-*H*), 5.85–5.82 (m, 4H, COT-*H*) ppm. ¹³C NMR (100.6 MHz, *d*₈-THF, 25 °C): δ = 98.1 (COT), 97.9 (COT), 95.9 (COT), 94.9 (COT), 72.4 (DME), 58.7 (DME), 1.4 (Si(CH₃)₃) ppm. ²⁹Si NMR (79.5 MHz, *d*₈-THF, 25 °C): δ = 0.8 ppm. MS (EI): *m/z* 672 (71%, [C₈H₆(SiMe₃)₂Lu + H]), 423 (64, [C₈H₆(SiMe₃)₂Lu]), 248 (64, [C₈H₆(SiMe₃)₂]), 207 (34, [C₈H₆(SiMe₃)₂-3Me]).

4.3 Preparation of the actinide sandwich complexes An(COT^{''})₂ (An = Th (9), U (10)) (general synthetic protocol)

~200 mg of anhydrous AnCl₄ (An = Th, U; ~0.5 mmol) were treated with 2.05 equiv. of freshly prepared Li₂(COT^{''}) in 25 mL of THF. Due to the high solubility of all reactants the reactions were finished after 2 h stirring at r.t. The solvent was evaporated and *n*-pentane (20 mL) was added, yielding an intense yellow solution (Th) and a red-green solution for the U complex **10**. Filtration and removal of the solvents afforded the crude complexes in ~80% yield. From the waxy yellow thorium complex **9** (m.p. 135 °C) single-crystals were obtained by recrystallization in a closed ampule at 240 °C under high vacuum. From the oily, crude uranium complex **10**, single-crystals grew in the refrigerator during storage at 4 °C for several months. Sublimation under identical conditions as described for Th led to the formation of red crystals in a green oil.

Th[C₈H₆(SiMe₃)₂]₂ (9). Elemental analysis calcd. for C₂₈H₄₈Si₄Th (*M_r* = 729.07 g mol⁻¹): C, 46.13; H, 6.64; Th, 31.83. Found: Th, 32.0%. IR (KBr disc): ν = 3036w, 3002m, 2954m, 2895m, 1447w, 1403w, 1382w, 1370w, 1330w, 1302w, 1249s, 1119w, 1051w, 1042w, 1018m, 988m, 964m, 926m, 838vs br, 812m, 806m, 780w, 750s, 720s, 710m, sh, 699w, 661w, 633m,

470w, 347m, 302m, 241m cm⁻¹. ¹H NMR (CDCl₃): δ = 6.86 (m, 12H, CH), 0.60 (br, 36H, CH₃) ppm. ¹³C NMR (CDCl₃): δ = 113.1, 112.3, 110.0 (CH), 0.9 (CH₃) ppm.

U[C₈H₆(SiMe₃)₂]₂ (10). Elemental analysis calcd. for C₂₈H₄₈Si₄U (*M_r* = 735.06 g mol⁻¹): C, 45.75; H, 6.58; U, 32.38. Found: U, 31.9%. IR (KBr disc): ν = 3031w, 2999m, 2956m, 2896m, 1586w, 1445w, 1403w, 1247s, 1081w, 1066w, 1038s, 977m, 940m, 931m, 900m, 838vs, br, 793w, 750s, 742m, 710m, sh, 691w, 651w, 633m, 540w, 502w, 478w, 458w, 422w, 338m, 303m, 283w, 249m cm⁻¹. UV-vis (Et₂O, λ , nm (ϵ , cm l mol⁻¹): 360, 380, 503, 520, 537, 567, 592(1461), 618(438), 635(195), 691(20), 732(19), 980(17), 1322(4), 1479(7), 1710(1), 1755(1), 1793(1), 1865(6) nm. ¹H NMR (CDCl₃): δ = -9.99 (36H, CH₃), -25.20 (4H, CH), -39.63 (4H, CH), -45.62 (4H, CH) ppm. ¹³C NMR (CDCl₃): δ = 325.9 (CH), 293.8 (CH), 270.3 (CH), -3.5 (CH₃) ppm.

4.4 Preparation of the actinide sandwich complexes An(COT^{''})₂ (An = Th (11), U (12))

The two polysilylated actinidocenes **11** and **12** were prepared by treatment of AnCl₄ (An = Th, U) with 2 equiv. of K₂(COT^{''}), following the procedure reported by Edlmann and Kanellakopoulos *et al.* (*cf.* Scheme 5).^{24b} Bright yellow **11** and dichroitic red/green **12** were isolated in high yields of around 80% after recrystallization from *n*-pentane.

4.5 Crystal structure determination

The intensity data of the lanthanide sandwich complexes **1–8** were collected on a Stoe IPDS 2T diffractometer with MoK α radiation. The data were collected with the Stoe XAREA program using ω -scans.³⁹ The space groups were determined with the XRED32 program. The structures were solved by direct methods (SHELXS-97) and refined by full matrix least-squares methods on *F*² using SHELXL-97.⁴⁰ Data collection parameters are summarized in Tables 1 and 2. Single-crystal X-ray analyses of the actinide complexes **9–12** were performed on a Bruker Apex II Quazar diffractometer at given temperature, collecting two or four spheres of data with an irradiation time of 10 to 40 s per frame, applying a combination of ω - and ϕ -scans. Maximum θ -values were in the range of 28°. Completeness of data to $\theta \leq 25^\circ$ was higher than 99%. For more information refer to Table 2. Integration of the data proceeded with SAINT,⁴¹ the data were corrected for Lorentz- and polarisation effects, and an experimental absorption correction with SADABS⁴¹ was performed. For searches relating to single-crystal X-ray diffraction data, the Cambridge Structural Database was used. The structures have been solved by direct methods and refined to a minimum *R*-value with SHELXL-2013⁴² *via* full-matrix least-squares on *F*². In the case of compound **9**, a second type of crystals could be isolated with a different elementary cell showing a strong disorder. The data have been deposited at the CCDC with the CCDC 1049928 but will not be discussed here in detail as due to the disorder the overall standard deviations for all values are significantly higher.



Acknowledgements

Financial support by the Otto-von-Guericke-Universität Magdeburg is gratefully acknowledged. Special thanks are due to Ms Desirée Schneider for preparing the ChemDraw Schemes.

References

- Review: F. T. Edelmann, Complexes of Scandium, Yttrium and Lanthanide Elements, in *Comprehensive Organometallic Chemistry III*, ed. R. H. Crabtree and D. M. P. Mingos, Elsevier, Oxford, 2006, p. 1.
- C. Meermann, K. Ohno, K. W. Törnroos, K. Mashima and R. Anwander, *Eur. J. Inorg. Chem.*, 2009, 76, and references cited therein.
- (a) F. Mares, K. O. Hodgson and A. Streitwieser, *J. Organomet. Chem.*, 1970, **24**, C68; (b) K. O. Hodgson, F. Mares, D. Starks and A. Streitwieser, *J. Am. Chem. Soc.*, 1973, **85**, 8650; (c) S. A. Kinsley, A. Streitwieser and A. Zalkin, *Organometallics*, 1985, **4**, 52; (d) A. L. Wayda, *Organometallics*, 1983, **2**, 565; (e) J. Jin, Z. Jin, G. Wei, W. Chen and Y. Zhang, *Chin. J. Inorg. Chem.*, 1993, **9**, 326; (f) U. Kilimann, M. Schäfer, R. Herbst-Irmer and F. T. Edelmann, *J. Organomet. Chem.*, 1994, **469**, C15; (g) S. Anfang, G. Seybert, K. Harms, G. Geiseler, W. Massa and K. Dehnicke, *Z. Anorg. Allg. Chem.*, 1998, **624**, 1187; (h) G. W. Rabe, M. Zhang-Presse, J. A. Golen and A. L. Rheingold, *Acta Crystallogr., Sect. E: Struct. Rep. Online*, 2003, **59**, m255.
- (a) F. Mares, K. O. Hodgson and A. Streitwieser, *J. Organomet. Chem.*, 1971, **28**, C24; (b) K. O. Hodgson and K. N. Raymond, *Inorg. Chem.*, 1972, **11**, 171; (c) K. O. Hodgson and K. N. Raymond, *Inorg. Chem.*, 1972, **11**, 3030; (d) A. L. Wayda, *Organometallics*, 1983, **2**, 565; (e) J. Xia, Z. Jin, G. Wei and W. Chen, *Jiegou Huaxue*, 1992, **11**, 113.
- (a) J. D. Jamerson, A. P. Masino and J. Takats, *J. Organomet. Chem.*, 1974, **65**, C33; (b) A. Westerhoff and H. J. De Liefde-Meijer, *J. Organomet. Chem.*, 1976, **116**, 319; (c) K. Wen, Z. Jin and W. Chen, *J. Chem. Soc., Chem. Commun.*, 1991, 680.
- A. Greco, S. Cesca and G. Bertolini, *J. Organomet. Chem.*, 1976, **113**, 321.
- (a) A. Streitwieser and S. A. Kinsley, in *Fundamental and Technological Aspects of Organo-f-Element Chemistry*, ed. T. J. Marks and I. L. Fragalà, NATO ASI Series, D. Reidel, Boston, 1985, vol. 155, p. 77; (b) A. Streitwieser and T. R. Boussie, *Eur. J. Solid State Inorg. Chem.*, 1991, **28**, 399; (c) F. T. Edelmann, *New J. Chem.*, 1995, **19**, 535; (d) F. T. Edelmann, *Angew. Chem., Int. Ed.*, 1995, **34**, 2466; (e) F. T. Edelmann, D. M. M. Freckmann and H. Schumann, *Chem. Rev.*, 2002, **102**, 1851; (f) H.-D. Amberger, F. T. Edelmann, J. Gottfriedsen, R. Herbst-Irmer, S. Jank, U. Kilimann, M. Noltemeyer, H. Reddmann and M. Schäfer, *Inorg. Chem.*, 2009, **48**, 760; (g) F. T. Edelmann, *New J. Chem.*, 2011, **35**, 517.
- K. Mashima and H. Takaya, *Tetrahedron Lett.*, 1989, **30**, 3697.
- (a) U. Kilimann, M. Schäfer, R. Herbst-Irmer and F. T. Edelmann, *J. Organomet. Chem.*, 1994, **469**, C10; (b) H. Schumann, J. Winterfeld, H. Hemling, F. E. Hahn, P. Reich, K.-W. Brzezinka, F. T. Edelmann, U. Kilimann, M. Schäfer and R. Herbst-Irmer, *Chem. Ber.*, 1995, **128**, 395; (c) U. Reißmann, P. Poremba, M. Noltemeyer, H.-G. Schmidt and F. T. Edelmann, *Inorg. Chim. Acta*, 2000, **303**, 156.
- (a) J. M. Bellama and J. B. Davidson, *J. Organomet. Chem.*, 1975, **86**, 69; (b) N. C. Burton, F. G. N. Cloke, P. B. Hitchcock, H. C. de Lemos and A. A. Sameh, *J. Chem. Soc., Chem. Commun.*, 1989, 1462; (c) N. C. Burton, F. G. N. Cloke, S. C. P. Joseph, H. Karamallakis and A. A. Sameh, *J. Organomet. Chem.*, 1993, **462**, 39.
- A. Streitwieser and U. Müller-Westerhoff, *J. Am. Chem. Soc.*, 1968, **90**, 7364.
- Review: D. Seyferth, *Organometallics*, 2004, **23**, 3562.
- (a) A. Hervé, N. Garin, P. Thuéry, M. Ephritikhine and J.-C. Berthet, *Chem. Commun.*, 2013, **49**, 6304; (b) J.-C. Berthet, P. Thuéry, N. Garin, J.-P. Dognon, T. Cantat and M. Ephritikhine, *J. Am. Chem. Soc.*, 2013, **135**, 10003.
- A. Edelmann, V. Lorenz, C. G. Hrib, L. Hilfert, S. Blaurock and F. T. Edelmann, *Organometallics*, 2013, **32**, 1435.
- V. Lorenz, A. Edelmann, S. Blaurock, F. Freise and F. T. Edelmann, *Organometallics*, 2007, **26**, 4708.
- V. Lorenz, S. Blaurock, C. G. Hrib and F. T. Edelmann, *Organometallics*, 2010, **29**, 4787.
- J. J. Le Roy, M. Jeletic, S. I. Gorelski, I. Korobkov, L. Ungur, L. F. Chibotaru and M. Murugesu, *J. Am. Chem. Soc.*, 2013, **135**, 3502.
- J. J. Le Roy, L. Ungur, I. Korobkov, L. F. Chibotaru and M. Murugesu, *J. Am. Chem. Soc.*, 2014, **136**, 8003.
- P. Poremba, U. Reißmann, M. Noltemeyer, H.-G. Schmidt, W. Brüser and F. T. Edelmann, *J. Organomet. Chem.*, 1997, **544**, 1.
- J. J. Le Roy, I. Korobkov, J. E. Kim, E. J. Schelter and M. Murugesu, *Dalton Trans.*, 2014, **43**, 2737.
- J. J. Le Roy, I. Korobkov and M. Murugesu, *Chem. Commun.*, 2014, **50**, 1602.
- V. Lorenz, A. Edelmann, S. Blaurock, F. Freise and F. T. Edelmann, *Organometallics*, 2007, **26**, 6681.
- M. Jeletic, P.-H. Lin, J. J. Le Roy, I. Korobkov, S. I. Gorelsky and M. Murugesu, *J. Am. Chem. Soc.*, 2011, **133**, 19286.
- (a) U. Kilimann, R. Herbst-Irmer, D. Stalke and F. T. Edelmann, *Angew. Chem., Int. Ed.*, 1994, **33**, 1618; (b) C. Apostolidis, F. T. Edelmann, B. Kanellakopulos and U. Reißmann, *Z. Naturforsch.*, 1999, **54b**, 960.
- A. Edelmann, S. Blaurock, V. Lorenz, L. Hilfert and F. T. Edelmann, *Angew. Chem., Int. Ed.*, 2007, **46**, 6732.
- A. Edelmann, C. G. Hrib, S. Blaurock and F. T. Edelmann, *J. Organomet. Chem.*, 2010, **695**, 2732.
- J. J. Le Roy, S. I. Gorelsky, I. Korobkov and M. Murugesu, *Organometallics*, 2015, **34**, 1415.
- (a) P. Poremba, H. G. Schmidt, M. Noltemeyer and F. T. Edelmann, *Organometallics*, 1998, **17**, 986; (b) M. Jeletic,



- F. A. Perras, S. I. Gorelsky, J. L. Le Roy, I. Korobkov, D. L. Bryce and M. Murugesu, *Dalton Trans.*, 2012, **41**, 8060.
- 29 (a) A. Avdeef, K. N. Raymond, K. O. Hodgson and A. Zalkin, *Inorg. Chem.*, 1972, **11**, 1083; (b) K. O. Hodgson and K. N. Raymond, *Inorg. Chem.*, 1973, **12**, 458; (c) L. K. Templeton, D. H. Templeton and R. Walker, *Inorg. Chem.*, 1976, **15**, 3000; (d) A. Zalkin, D. H. Templeton, S. R. Berryhill and W. D. Luke, *Inorg. Chem.*, 1979, **18**, 2287; (e) A. Zalkin, D. H. Templeton, W. D. Luke and A. Streitwieser Jr., *Organometallics*, 1982, **1**, 618; (f) A. Zalkin, D. H. Templeton, R. Kluttz and A. Streitwieser Jr., *Acta Crystallogr., Sect. C: Cryst. Struct. Commun.*, 1985, **41**, 327.
- 30 V. Lorenz, B. M. Schmiede, C. G. Hrib, J. W. Ziller, A. Edelmann, S. Blaurock, W. J. Evans and F. T. Edelmann, *J. Am. Chem. Soc.*, 2011, **133**, 1257.
- 31 (a) H. P. Fritz, *Adv. Organomet. Chem.*, 1964, **1**, 239; (b) L. Hocks, J. Goffart, G. Duyckaert and P. Teyssie, *Spectrochim. Acta, Part A*, 1974, **30**, 907; (c) V. T. Aleksanyan, I. A. Garbusova, T. M. Chernyshova, Z. V. Todres, M. R. Leonov and N. I. Gramateeva, *J. Organomet. Chem.*, 1981, **217**, 169.
- 32 (a) A. Streitwieser and U. Müller-Westerhoff, *J. Am. Chem. Soc.*, 1973, **95**, 8644; (b) R. Bohlander, PhD thesis, University of Karlsruhe, 1986; (c) N. Magnani, C. Apostolidis, A. Morgenstern, E. Colineau, J.-C. Griveau, H. Bolvin, O. Walter and R. Caciuffo, *Angew. Chem., Int. Ed.*, 2011, **50**, 1696.
- 33 C. R. Graves, A. E. Vaughn, E. J. Scheluter, B. L. Scott, J. D. Thompson, D. E. Morris and J. L. Kiplinger, *Inorg. Chem.*, 2008, **47**, 11879, and references cited therein.
- 34 (a) A. Streitwieser, Jr., R. Q. Kluttz, K. A. Smith and W. D. Luke, *Organometallics*, 1983, **2**, 1873; (b) W. Jahn, K. Yünlü, W. Oroschin, H.-D. Amberger and R. D. Fischer, *Inorg. Chim. Acta*, 1984, **95**, 85; (c) A. Streitwieser Jr., M. H. Lyttle, H.-K. Wang, T. Boussie, A. Weinländer and J. P. Solar, *J. Organomet. Chem.*, 1995, **501**, 245.
- 35 (a) A. W. Spiegl, Doctoral dissertation, University of Erlangen-Nürnberg, 1978; (b) R. D. Fischer, NMR-spectroscopy of Organo-f-Element and Pre-Lanthanoid Complexes: Some Current Trends, in *Fundamental and Technological Aspects of Organo-f-Element Chemistry*, ed. T. J. Marks and I. L. Fraga, and D. Reidel Publishing Company, 1985, pp. 277–326.
- 36 J. H. Freeman and M. L. Smith, *J. Inorg. Nucl. Chem.*, 1958, **7**, 224.
- 37 D. C. Bradley, M. A. Saad and W. Wardlaw, *J. Chem. Soc.*, 1954, 2002.
- 38 J. A. Hermann, J. F. Suttle and H. R. Hoekstra, *Inorg. Synth.*, 1957, **5**, 143.
- 39 Stoe, *XAREA, Program for X-ray Crystal Data Collection*, (XRED32 included in XAREA) Stoe, 2002.
- 40 (a) G. M. Sheldrick, *SHELXL-97 Program for Crystal Structure Refinement*, Universität Göttingen, Germany, 1997; (b) G. M. Sheldrick, *SHELXS-97 Program for Crystal Structure Solution*, Universität Göttingen, Germany, 1997.
- 41 Bruker APEX, *SAINTE, SADABS, programs for X-ray Crystal Data Collection, integration and absorption correction*, Bruker AXS Inc., Madison, Wisconsin, USA, 2007.
- 42 G. M. Sheldrick, *Acta Crystallogr., Sect. A: Found. Crystallogr.*, 2008, **64**, 112.

